

Figure 1
Burstein et al.
ApJS 1996/7

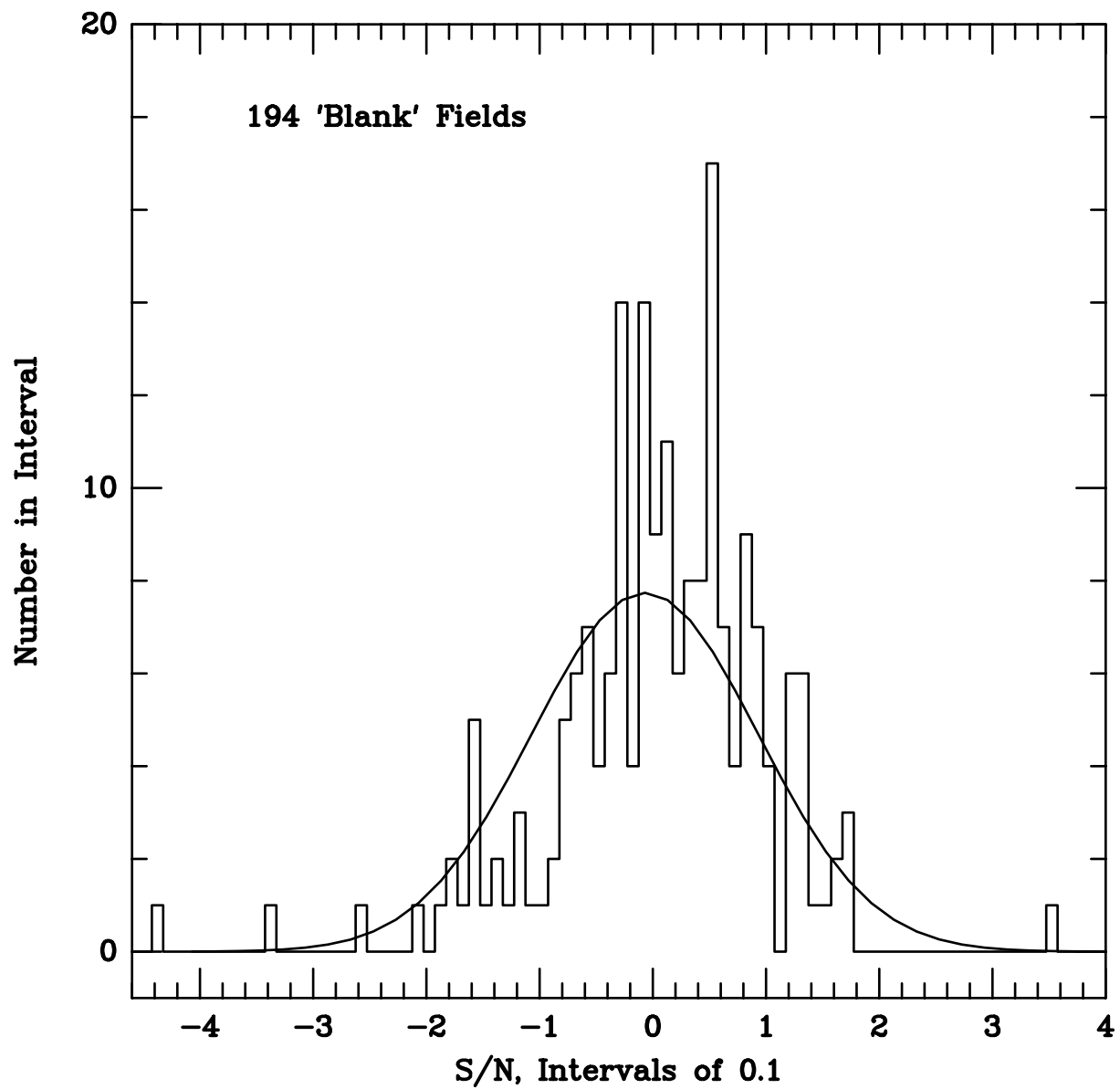


Figure 2
Burstein et al.
ApJS 1996/7

S/N Distributions for E, S0, E/S0 Galaxies, by Catalog

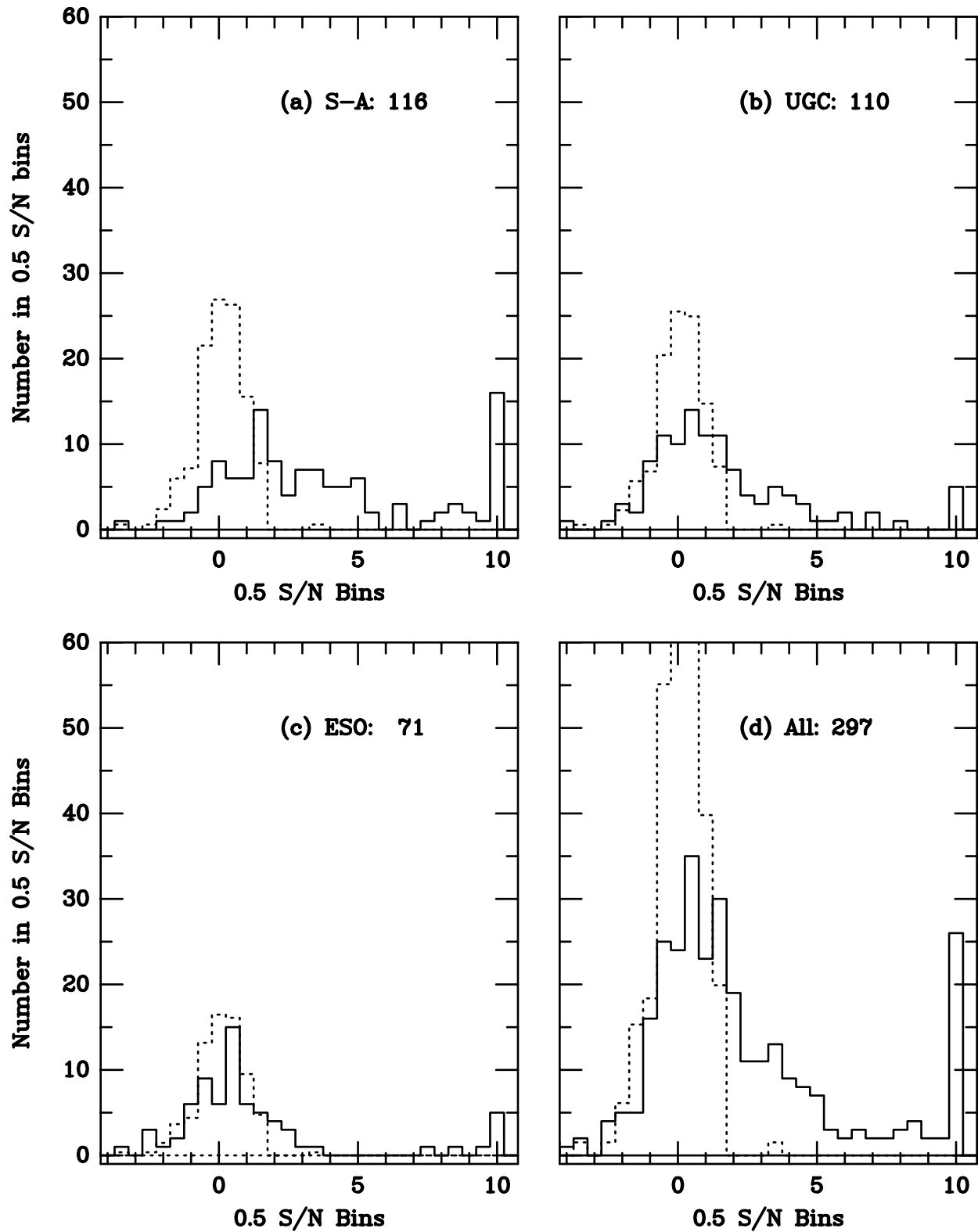


Figure 3
Burstein et al.
ApJS 1996/7

S/N Distributions for Spiral and Irregular Galaxies, by Catalog

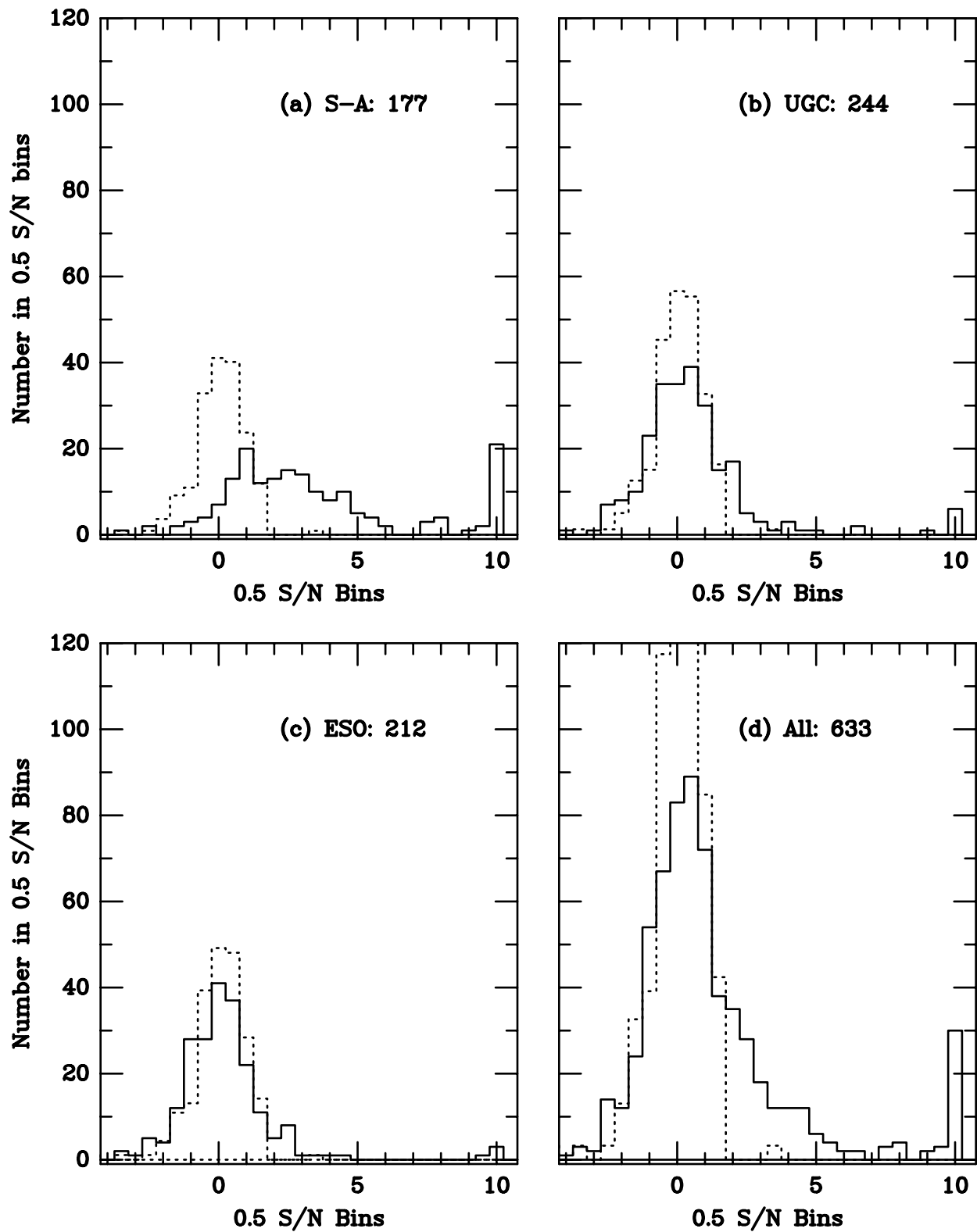


Figure 4
Burstein et al.
ApJS 1996/7

Table 1: Reasons for Exclusion of Galaxies from X-ray measurements

Catalog	On 'Ribs'	Near Edge of IPC Field	In Diffuse Emission	In S-A Catalog	HRI only	Image not usable
UGC	116	86	52	103	19	4
ESO	133	82	126	72	10	22
S-A*	27	16	33	—	4	—

* 11 galaxies in S-A sample also excluded for being too large for adequate coverage with survey apertures.

 Table 2: Conversion of X-ray count rate (1 IPC ct/sec) to 0.5 - 4.5keV flux (ergs/cm²/sec x 10⁻¹¹)

HI column density (10 ²⁰)	X-ray correction factor
30.0	5.376
20.06	4.718
13.41	4.280
8.963	3.977
5.992	3.752
4.006	3.571
2.678	3.420
1.790	3.293
1.197	3.188
0.800	3.103

Table 3: Number of Galaxies for Which Given Aperture is the Largest Observed

Aperture	200"	232"	264"	296"
UGC	10	35	25	323
ESO	27	47	11	227
S-A	3	10	7	293

Table 4: Corrections to aperture measurements used to estimate total X-Ray fluxes

Source type	200" aperture correction	232" aperture correction	264" aperture correction	296" aperture correction
Ellipticals/diffuse gas	1.44	1.27	1.16	1.07
Spirals	1.10	1.05	1.01	1.00 ^a
Point sources/Seyferts	1.08	1.05	1.03	1.01 ^a

^a Difference between spiral and point source arises from uncertainties and the difference is not significant.

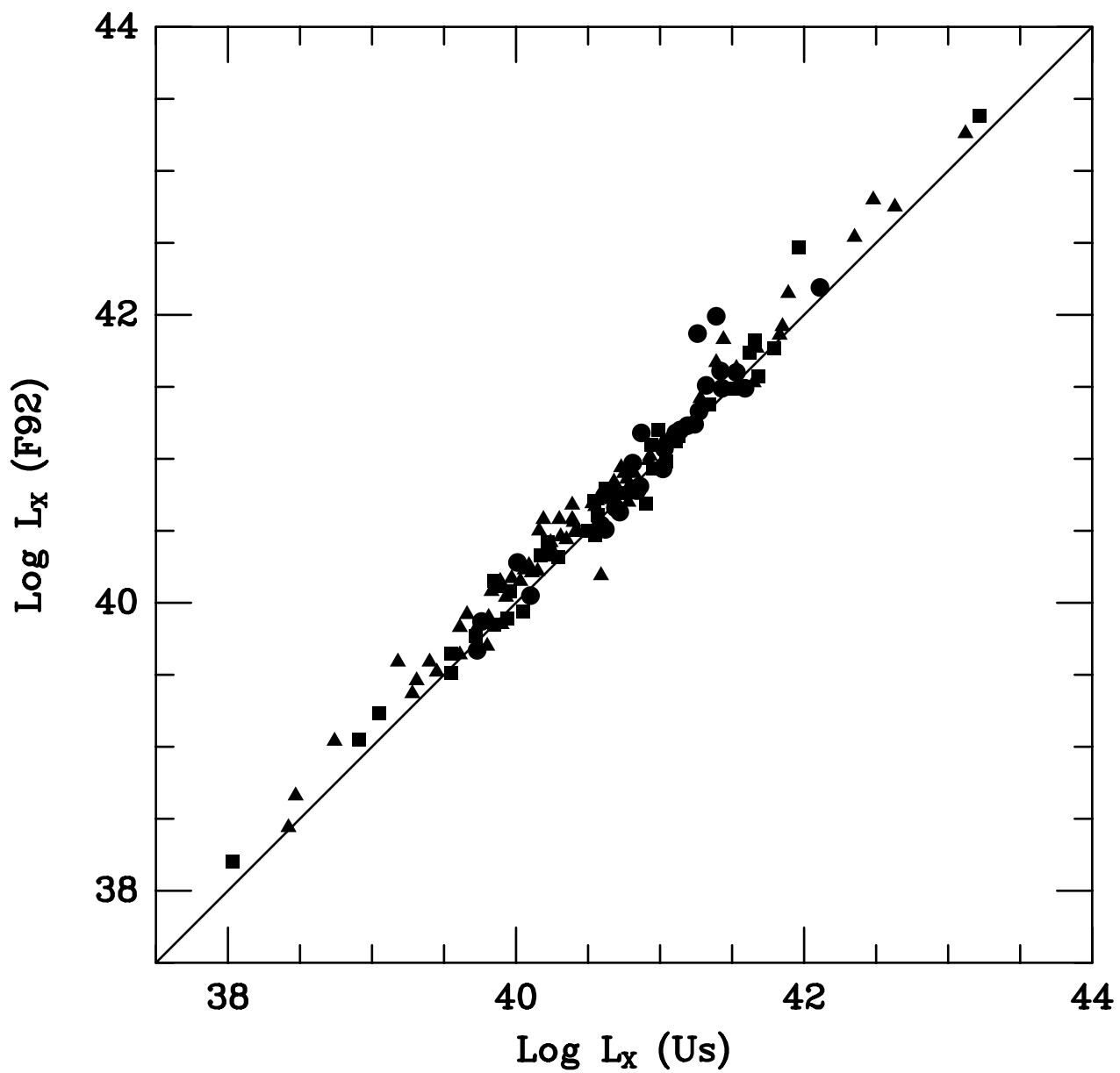


Figure 5
Burstein et al.
ApJS 1996/7

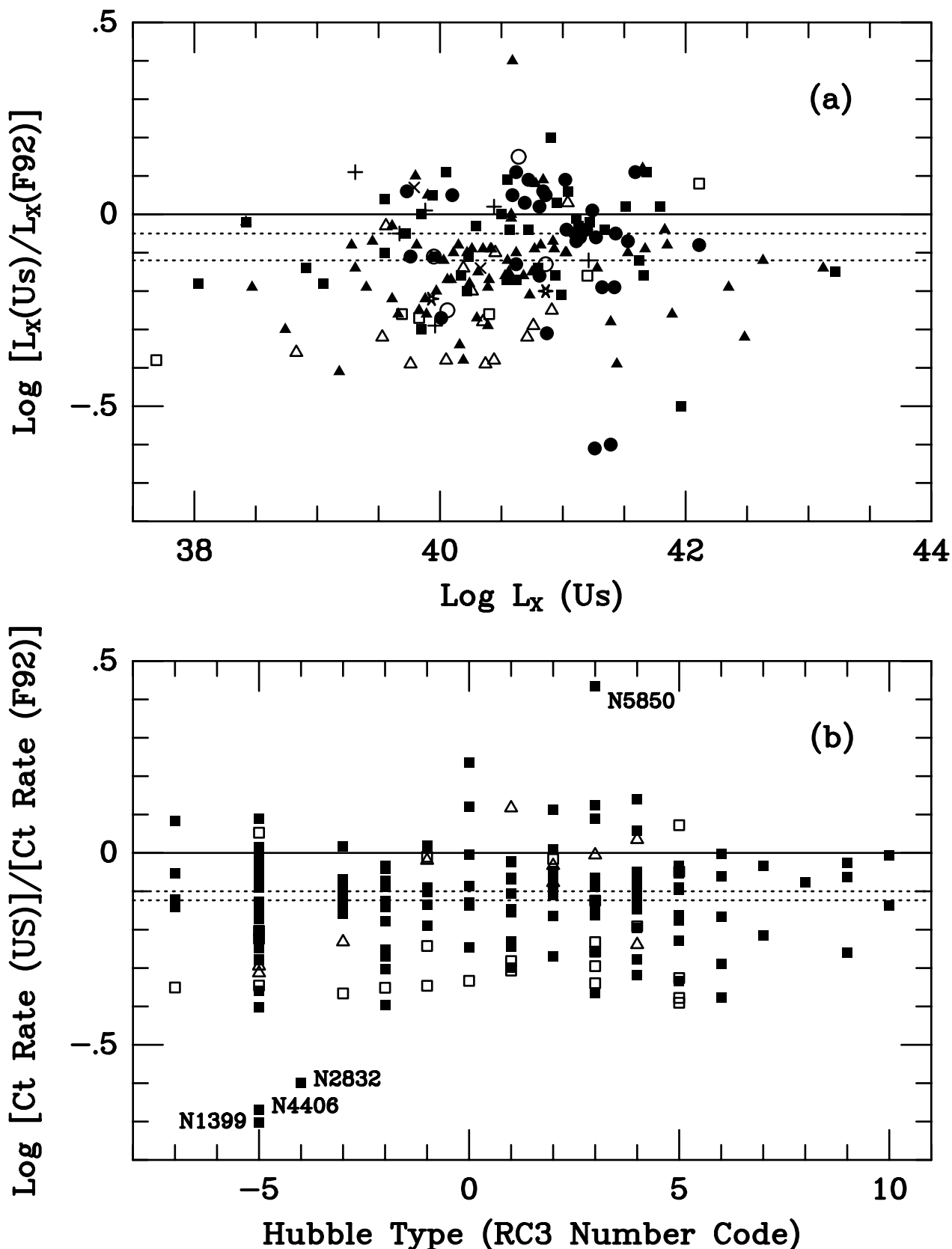


Figure 6
Burstein et al.
ApJS 1996/7

An Einstein X-ray Survey of Optically-Selected Galaxies: I. Data

David Burstein

Dept. of Physics & Astronomy, Arizona State University, Tempe, AZ

Email: burstein@samuri.la.asu.edu

C. Jones, W. Forman

Harvard-Smithsonian Center for Astrophysics, Garden St., Cambridge, MA 02138

Email: cjf@cfa236.harvard.edu, wrf@cfa.harvard.edu

A. P. Marston

Dept. of Physics & Astronomy, Drake University, Des Moines, IA 50311

Email: tm9991r@acad.drake.edu

Ronald O. Marzke

Harvard-Smithsonian Center for Astrophysics, Garden St., Cambridge, MA 02138

and

Dominion Astrophysical Observatory, Herzberg Institute of Astrophysics

National Research Council of Canada

5071 W. Saanich Rd., Victoria, BC, Canada V8X 4M6

Email: marzke@dao.nrc.ca

ABSTRACT

We present the results of a complete Einstein Imaging Proportional Counter (IPC) X-ray survey of optically-selected galaxies from Shapley-Ames Catalog, Uppsala General Catalog and the European Southern Observatory Catalog. Well-defined optical criteria are used to select the galaxies, and X-ray fluxes are measured at the optically-defined positions. The result is a comprehensive list of X-ray detection and upper-limit measurements for 1018 galaxies. Of these, 827 have either independent distance estimates or radial velocities. Associated optical, redshift and distance data has been assembled for these galaxies, and their distances come from a combination of directly predicted distances and those predicted from the Faber-Burstein Great Attractor/Virgocentric infall model.

The accuracy of the X-ray fluxes has been checked in three different ways; all are consistent with the derived X-ray fluxes being of ≤ 0.1 dex accuracy. In particular, there is agreement with previous published X-ray fluxes for galaxies in common with Roberts et al. (1991) and Fabbiano et al. (1992). The data

presented here will be used in further studies to characterize the X-ray output of galaxies of various morphological types and thus to enable the determination of the major sources contributing to the X-ray emission from galaxies.

1. Introduction

Almost all X-ray surveys of galaxies published to date have used galaxy samples chosen on the basis of apparent optical brightness. These include the first surveys of the HEAO-2 (Einstein) data base (Long & Van Speybroeck, 1981; Forman, Jones & Tucker, 1985; Fabbiano & Trinchieri, 1987; Canizares, Fabbiano & Trinchieri, 1987, and references therein; Roberts et al. 1991), as well as the compilation by Fabbiano et al. (1992; hereafter F92). In total 405 galaxies have Einstein measurements of X-ray properties studied in these surveys, all chosen from either the Shapley-Ames Catalog (Shapley & Ames 1932; hereafter S-A) or the Second Catalog of Bright Galaxies (de Vaucouleurs, de Vaucouleurs & Corwin 1976; here after RC2). As analyzed by F92, 207 of these galaxies have 3σ X-ray detections.

However, consider the analogy with stars: The H-R diagram of the 100 brightest stars in the sky is very different from that of the 100 nearest stars. Is it possible that the same kinds of differences occur in galaxy samples similarly chosen, with the additional option that galaxies can be selected either by apparent brightness or by apparent size? A direct answer to this question is needed for a physical property of galaxies such as X-ray flux. The X-ray flux can come from several different sources within a given galaxy (e.g., hot thermal gas; accretion disks around binaries; central engines of active galaxies).

Given this motivation, the observational goal of the present survey was to obtain measurements of the X-ray flux (or upper limits) at the positions of galaxies optically-selected in two different ways, as viewed in the Imaging Proportional Counter (IPC) fields obtained by the Einstein Observatory. One set, from the S-A catalog, is selected on the basis of apparent magnitude. Two data sets, one from the Uppsala General Catalog (Nilson 1973; hereafter UGC) and European Southern Observatory catalog (Lauberts 1982; hereafter ESO) are chosen on the basis of apparent size.

In the present paper, we present the X-ray measurements we made and the associated optical, redshift and distance data for 1018 galaxies. A second paper will analyze the global properties of galaxies as found by this survey. § 2 discusses how the galaxies were selected for study, and how the X-ray data were obtained. In § 3 we discuss the origin of the non-X-ray data used for the

galaxies in this survey — radial velocities, distances, magnitudes and diameters. Many of the normal galaxies with published X-ray fluxes from Einstein fields have had their X-ray fluxes independently determined by this survey, in order to permit ready correspondence to previous results. Tests of the uniformity of the X-ray data are detailed in § 4, including a detailed comparison with the F92 published X-ray counts and fluxes. § 5 gives a summary of the paper.

2. Galaxy Selection and Einstein X-ray Observations

2.1. Combined Optical/X-ray Selection of Galaxies

Most tests of the inclination-dependence of the observed properties of galaxies show that while the magnitudes of E and S0 galaxies are inclination-invariant, those of spiral galaxies are inclination-dependent (cf. Burstein, Haynes & Faber 1991). This difference is due to the fact that spiral galaxies have visible dust distributed in their disks (cf. Giovanelli 1995), while the dust seen in E and S0 galaxies is well-known to be localized near their centers. Specific tests on the UGC-measured and ESO-measured diameters of spiral galaxies indicate little change with inclination (e.g. Valentijn 1990; Burstein et al. 1991). However, interpreting these tests in terms of whether spiral galaxies actually have inclination-independent isophotal diameters is still in debate (cf. Davies, Jones & Trehella 1995; Burstein, Willick & Courteau 1995; Giovanelli 1995).

Nevertheless, it is clear that the inclination-dependencies of magnitudes and diameters for E/S0's is different from that for spiral and irregular galaxies. As such, it is not surprising that their relative numbers are different in a magnitude-limited sample (spirals undersampled), relative to a diameter-limited sample (spirals oversampled). One finds that galaxies of types E, S0 and S0/a comprise 24% of the S-A catalog (Sandage & Tamman 1981), while such galaxy types comprise only 16% of either the UGC or ESO catalogs. The present X-ray survey includes galaxies from all three catalogs, as one check for inclination-dependent selection effects influencing the results of X-ray studies of galaxies. Taken together, the data from all three catalogs comprises the most complete survey one can do for the brightest galaxies with the Einstein data base.

The methodology we employ is to use the optical positions of galaxies to locate apertures of known size at the corresponding locations in the Einstein images, and then to measure the observed count rate within these apertures, properly correcting for background count rate. As we expect to find upper limits to the fluxes of most galaxies, the need for accurate detection statistics

make the use of relatively long exposures desirable. A lower exposure limit of 2000 seconds was chosen for images obtained with the Imaging Proportional Counter (IPC) for UGC and ESO galaxies, and a lower limit of 1500 seconds was used for S-A galaxies (owing to the fact that the S-A galaxies are, in general, closer and generally of higher flux than the UGC and ESO galaxies). After some experimentation, High Resolution Imager (HRI) exposures were not used for the final sample as the lower sensitivity of the HRI yielded much higher signal-to-noise upper limits, on average.

Galaxy selection for the present samples proceeded by cross-correlating the galaxy positions in each catalog with the positions of all Einstein IPC fields with at least the minimum exposure time. Each IPC pixel is 8 arc-sec on a side, hence galaxy positions accurate to ≈ 10 arc-sec are sufficient for the purposes of this survey. Galaxies in the ESO and S-A catalogs have positions generally this accurate, and their quoted positions were used directly in the cross-correlation with IPC image positions.

Galaxies in the UGC have positions of mixed accuracy, some of which are very poor (> 1 arc-minute). Improved positions for UGC galaxies were obtained in a two-step process: First, a cross-correlation was done between UGC-listed galaxy positions and IPC field positions. After further objective selection criteria were applied (common to all three catalogs and discussed below), a final list of 773 UGC galaxies was compiled. Second, accurate positions were either obtained from Dressel & Condon (1976) (320 of their 1800 galaxies are in our sample), or were measured by one of us (ROM) in the following manner: Transparent overlays were made of the field around the UGC position of each galaxy, to the scale of the Palomar Sky Survey (PSS) prints. Star positions and the UGC galaxy position were marked, and the direction of N-S and E-W drawn. This overlay was then placed on the PSS print, and the position of the galaxy on the print, relative to the UGC position, was measured with a graduated reticle in both Right Ascension and Declination. Comparison with 35 positions measured by Dressel & Condon indicate that the positions for 454 galaxies measured in this manner are accurate to ± 12 arc-seconds, adequate for the purposes of this survey. A post-survey re-comparison with the UGC indicates that we missed at most 15 galaxies (for reasons such as bad search positions; IPC image not yet processed, etc.) that could otherwise have been in our survey. This omission has a negligible effect on the results of this survey.

Three optical selection criteria are applied to all three catalogs: galaxies with galactic reddenings, $E(B-V) > 1.00$ (from Burstein & Heiles 1984 and unpublished) were excluded, as well as galaxies without a listed morphological

type. Galaxies with listed optical diameters larger than $5'$ are excluded from the UGC and ESO catalogs, but not necessarily from the S-A catalog. Multiple galaxies listed in the UGC and ESO catalogs are included in this survey. X-ray selection criteria are discussed below.

The combination of optical and X-ray selection criteria results in 773 UGC galaxies in 483 IPC fields, 757 ESO galaxies in 232 IPC fields and 404 S-A galaxies in 374 IPC fields. Of the 773 UGC galaxies, 103 are also in the S-A catalog; of the 757 ESO galaxies, 72 are in the S-A catalog. This survey therefore includes a total of 1759 galaxies with 2147 galaxy observations in 942 IPC fields (97 of these galaxies had X-ray counts measured by more than one of us independently). In addition, 194 measurements are taken at random positions in 8% of the IPC fields (see § 2.2).

2.2. X-Ray Flux Determinations

In obtaining the raw counts for the source and background regions from the IPC images, we used the energy range from 0.56 to 4.47 keV. Four box apertures are employed for measuring source counts, having sizes of $200''$, $232''$, $264''$ and $296''$ on a side. The size of the largest aperture was dictated by the necessity of uniformly measuring many galaxies in arbitrary positions on the IPC images.

The X-ray source and background counts on the IPC images were visually examined using the HEAO Image Processing monitor. Each IPC image was displayed and the position of each galaxy marked on the field. As with photoelectric aperture photometry of galaxies, in measuring background count rate, care was taken to avoid regions where the background was high, varying spatially, or where the IPC image was obstructed by the detector window support structure ('rib').

If the galaxy position lay close to a 'rib', or close to the edge of the field, the smaller apertures were measured if they could yield good data. However, in the majority of cases, placement near a 'rib' or near the edge of the field meant that counts could not be measured for the galaxy. If the galaxy position lay within a region of diffuse emission (such as exists in a galaxy cluster), the galaxy was similarly excluded from X-ray measurement. Table 1 gives the numbers of galaxies rejected and the reasons for rejection. Background count rates were measured for each galaxy, both near the galaxy location and at 'mirror-image' positions on the same field, after confirming that the background positions did not contain any obvious X-ray sources.

Two internal checks of our measuring procedure are made during the course

of this survey. First, measurements are made at the positions of 194 'blank' fields, using the same procedures as for the sample galaxies. These fields are chosen in 73 IPC images that sample the range of exposure times used in this survey. The data for these 'blank' fields are then processed in the same manner as for the galaxies. Second, due to the labor-intensive, interactive manner of deriving the aperture measurements, it is desirable that a subset of the galaxies be measured twice, once each by different "observers". The IPC emission of 97 galaxies were measured twice, once during the UGC/ESO phase of the program and once later during the S-A phase. Comparison of the two sets of observations yield very close agreement. In order to preserve similar signal-to-noise, we do not average these two separate measurements of the same IPC image, but rather use just one.

X-ray fluxes are computed from the IPC images by correcting the net source counts in each aperture measured for the following explicit issues: a) the exposure time; b) the instrument deadtime ($\sim 4\%$); c) telescope vignetting (Harris *et al.* 1991); d) HI column density; e) spectral energy distribution of the source; and f) predicted ratio of flux within measured aperture to total flux. The first three corrections are well-known; for the vignetting corrections we assume a mean photon energy of 1.49 keV.

The next two corrections require knowledge of the HI column density (taken from Stark *et al.* 1992 and sources given in Marshall & Clark 1984) and the spectral energy distribution of the source. As the total number of counts for even the detected galaxies in our sample is generally too small to constrain the energy spectrum, we must assume a spectral energy distribution for these galaxies. As a test, we compare the differences in conversion rates that would arise from three different forms of the spectrum: a) a 1 keV Raymond spectrum as appropriate for luminous ellipticals; b) a 7 keV exponential spectrum as characteristic of binary X-ray sources; and c) a power law spectrum with a photon index of 1.5 typical of AGN. For each kind of spectrum we generate the count rate to flux conversion for a range of HI values from 8×10^{19} to 3×10^{21} $\text{N}_\text{H} \text{cm}^{-2}$. The hard exponential and power law spectra give nearly the same count rate to flux conversions. The ratio of the 1 keV thermal conversion value to the other conversions ranges from 0.75 for low HI column density to 0.85 for high HI.

However, the X-ray emission mechanism for each galaxy, or even each type of galaxy is not certain. For example, although binary sources are found in spiral galaxies, at least some spirals also have substantial diffuse emission. While hot gas seems to dominate the X-ray emission from ellipticals, many X-ray

detected early-type galaxies contain active galaxy nuclei. Thus, at this stage in our analysis, we are reluctant to assign a particular spectrum to a particular class of galaxy and thereby bias the flux conversions. Instead we choose to use an average count rate to flux conversions dependent only on the galactic HI column density, as given in Table 2 for all the galaxies in our samples, which is a compromise among the results from the three models.

The aperture-related correction is necessary as some galaxies could have fluxes only determined in smaller apertures. Smaller apertures are used when a source is near the edge of the field, near a rib, or near another source. Hence, data from all four X-ray apertures are used to examine the spatial distribution of the X-ray sources that are detected. Growth curves calculated from bright X-ray sources were used to extrapolate the flux from the largest aperture available for each galaxy observation, to a total flux. These corrections, listed in Table 3, are computed separately for elliptical galaxies, spiral galaxies and central point source-dominated galaxies (such as Seyfert galaxies). Table 4 gives the number of galaxy observations for which each aperture was the largest measured. X-ray fluxes for 82% of the UGC galaxies with X-ray observations, 75% of the ESO galaxies, and 94% of the S-A galaxies are measured in the largest aperture used in this survey (296" on a side). For those galaxies whose measured aperture is a smaller aperture, the observed flux in that smaller aperture is corrected to that of the largest aperture using the ratios in Table 3.

Signal-to-noise is calculated in the usual manner assuming a Gaussian distribution of errors and taking into account both galaxy and background measurements. From our accuracy tests (see below), a signal-to-noise ratio of 2.5 was chosen to distinguish between X-ray detections and non-detections in this sample. If a galaxy has $S/N \geq 2.5$, the flux given is the flux observed. If a galaxy has $S/N < 2.5$, the flux given is $2.5 \times N$.

Finally, it should be clear that, although the selection of galaxies was done in an objective manner, only 5% of the sky is covered by IPC images. As many galaxies are IPC targets, the net effect is to incorporate a combination of several selection effects. We keep track of this effect by the size of the vignetting correction, which is close to unity for objects near the center of the Einstein IPC images. In the cases for galaxies observed on more than one IPC image, the vignetting correction value closest to unity are kept.

The number of galaxies included in this survey, relative to the total number of galaxies in the relevant optical catalogs is shown in Figure 1. Galaxies are divided into four sections by morphological class: ellipticals and S0's, early-type spirals, late-type spirals and irregulars, and others (e.g. dwarfs, peculiars,

multiple galaxies). This last category was used only for the UGC and ESO catalogs. Within each class, in Figure 1 we plot the fraction of galaxies included in the X-ray sample compared to those available from the whole catalog as a function of either apparent size (UGC and ESO) or apparent magnitude (S-A).

As is evident, the percentage of galaxies in the S-A sample with measured X-ray fluxes is an order of magnitude higher than in the diameter-selected sample. Yet, due to the order of magnitude higher number of galaxies included in the UGC and ESO catalogs, the total number of galaxies with measured X-ray fluxes is comparable in each catalog. Within statistical fluctuations, the X-ray observed samples are fair cross-sections of both morphological types and apparent size (or magnitude) for these three catalogs.

3. Optical, Redshift and Distance Data

3.1. Optical Data

Optical diameters, magnitudes and axial ratios for blue magnitude data are given for each galaxy in this survey when available. The primary source for the S-A sample is the RC2, for which apparent magnitudes (either on the Harvard corrected system, or on the BT system) are given, together with isophotal diameters (to the 25th mag isophote) and axial ratios. UGC galaxies have optical data obtained primarily from the UGC, for which diameters, axial ratios and magnitudes are listed. UGC galaxy magnitudes that are 15.7 or brighter come from the Zwicky *et al* (1961) catalog. Zwicky magnitudes require correction to be placed on a common system in reasonable accord with the RC2 system. The correction procedure adopted here is that advocated by Huchra (1976).

ESO galaxies have optical data obtained from the more recent photographic surface photometry published by Lauberts & Valentijn (1988). This photometry is available for 85% of the original 16,154 galaxies in the ESO survey and, as such, is available for a similar percentage of the galaxies in the present survey. The 25th blue magnitude isophotal diameters and total blue magnitudes used here are taken from Lauberts & Valentijn; axial ratios are taken from the original ESO catalog (Lauberts 1982).

Galactic reddenings, $E(B-V)$ are taken from Burstein & Heiles (1984) for the RC2 and UGC galaxies, and separately calculated using the Burstein-Heiles reddening maps for ESO galaxies. The reddenings are expressed in terms of Burstein-Heiles-defined galactic extinction, $A_B = 4 \times E(B-V)$. Redshift-dependent K-corrections are calculated using the precepts of the RC2.

3.2. Redshifts and Distances

Heliocentric radial velocities are obtained primarily from the computer-readable version of the Third Reference Catalog of Bright Galaxies (de Vaucouleurs et al. 1991; hereafter RC3), as distributed by H.G. Corwin, Jr. These values are then supplemented by examination of the NASA Extragalactic Database (NED), as of February, 1996.

Distances for galaxies are determined in a two-step process. First, all of the galaxies in this sample are cross-correlated with the galaxies in the Mark III Catalog of Galaxy Peculiar Velocities (Willick et al. 1995; 1996a,b; references cited in notes to Table 7). We use the distances termed “inhomogeneous Malmquist-corrected” as given in the Mark III. Distances of galaxies are expressed in km sec^{-1} units, using $H_0 = 75 \text{ km sec}^{-1} \text{ Mpc}^{-1}$. Galaxies without directly measured distances, but with measured radial velocities have their distances calculated, in terms of km sec^{-1} , by the Great Attractor velocity field model of Faber & Burstein (1988).

3.3. The Observed and Derived Data Sets

Tables 5a, b and c contain the observed data for this survey for the galaxies in the UGC, ESO and S-A catalogs, respectively. Only those galaxies with X-ray measurements are included. This includes 313 S-A galaxies, 393 UGC (not S-A) galaxies and 312 ESO (not S-A) galaxies, for a total of 1018 galaxies with X-ray observations. These have the following format: Column (1) gives the name of the galaxy; column (2) the apparent blue magnitude of the galaxy; column (3) the logarithm of the blue isophotal diameter; column (4) the morphological type number, T (as explained in the notes to this Table). Column (5) gives the Einstein field number used for the X-ray data. A value of -1 indicates that multiple fields were used (see Table 8 for a listing of these fields). Column (6) gives the total exposure time for this galaxy (including all IPC images sampled). Columns (7) and (8) give the RA (1950) and Dec (1950) position at which the X-ray image was searched. Column (9) gives the X-ray count rate measured for this galaxy, in units of 1000 times the observed count rate. This count rate is only corrected for background and deadtime correction. Column (10) gives the error on this count rate, in the same units. The values in Column (11) are the multipliatiive IPC count rate to flux conversion for the energy range from 0.5 to 4.5 keV for an IPC count rate of 1 count/second and an X-ray spectrum, as discussed in section §2.2. Column (12) contains the IPC vignetting correction. If more than one IPC image is used for the observed

count rate, the vignetting correction given here is the exposure-weighted average of the individual vignetting corrections. Column (13) indicates which of the four apertures were used to obtain the observed count rate (1 = smallest, 4 = largest).

Tables 6a, b and c list those galaxies included in the original survey, but for which X-ray measurements were not made. The reasons for exclusion (discussed in more detail previously in § 2.2) include obscuration by the ‘ribs’ of the IPC; near or off the edge of the IPC image; only in HRI images; or within diffuse X-ray emission. Eleven S-A galaxies that were too large for the apertures used in this survey also were not observed. In Tables 6, column (1) has the name of the galaxy; column (2) the apparent blue magnitude of the galaxy (if available); and column (3) the numerical code indicating the reason for omission (see notes to the tables for an explanation of this code.)

Tables 7a,b,c contain the distance-dependent derived parameters for the X-ray measured galaxies in this survey. Column (1) gives the galaxy name; column (2) the heliocentric radial velocity. Column (3) gives the distance used for this galaxy, in units of Mpc (assuming $H_0 = 75 \text{ km sec}^{-1} \text{ Mpc}^{-1}$), while column (4) gives a numerical code for the source of this distance, as detailed in the table notes. Columns (5), (6) and (7) give the absolute B magnitude, log of galaxy diameter (in kpc) and fully-corrected absolute X-ray luminosity for this galaxy. Column (8) notes which galaxies are generally classified as Seyfert galaxies. Tables 7 include 329 UGC galaxies, 180 ESO galaxies and all 313 S-A galaxies, for a total of 822 galaxies (81% of the total sample) with both X-ray observations and known distances. The 196 galaxies in the UGC and ESO samples that have measured X-ray fluxes (both detected and upper limits), but do not yet have radial velocity measurements are given in Table 9. Included among these are 11 galaxies whose X-ray emission was detected with Einstein.

4. Internal and External Estimates of the Accuracy of the X-ray Data

4.1. Sky Measurements and ‘Blank’ Fields

For 251 of the 1018 galaxies with X-ray measurements (24.7%), the observed X-ray flux has a signal-to-noise (S/N) of 2.5 or better and a redshift is known. Correcting this percentage for the number of false detections, which we determined through a similar analysis of “blank” fields, we have a detection rate of 22.6%. Most of the galaxies in this survey have only X-ray upper limit values. The fact that most galaxies in this survey would not be detected at a significant

level was expected at the outset. Indeed, one of the principal aims of this survey was to assemble enough galaxies in each morphological class so that an average X-ray flux per class could be derived, even if most individual galaxies were not detected. Given this intent, it was important to be able to verify the statistical accuracy of noise estimates.

This was done in two ways. First, the 194 blank fields were measured. As noted above, these were treated in the same way as the galaxy measurements. S/N histograms from the blank field observations were compared to those formed from the program galaxies. Second, comparisons were made among the 97 galaxies which were twice measured independently.

Figure 2 shows the histogram of the S/N measurements of the blank field measurements. Also plotted in this histogram is the expected Gaussian distribution of S/N. There is a slight tendency for the blank fields to show a small net positive S/N (+0.095) compared to a Gaussian distribution. Nevertheless, the measurement of these blank fields is not expected to produce a Gaussian distribution based at $S/N = 0$, but rather be representative of what we would have measured in the absence of X-ray flux at these galaxy positions.

In Figures 3 and 4 we show X-ray measurement signal-to-noise distributions for E/S0 galaxies (Figure 3) and spiral and irregular galaxies (Figure 4) separately for the three catalog samples, and for all of the data together. Plotted over these histogram distributions is the measured distribution for the blank fields, scaled to match the number of galaxies actually measured in each sample. It is satisfying that the negative S/N tail of the blank fields defines the minimum S/N of all of the galaxy samples in which most galaxies are not detected. This is particularly true for spiral and irregular galaxies, and gives us confidence in the accuracy of our measurements.

The histograms in Figures 3 and 4 show two trends. First, it is obvious that almost all of the S-A galaxies have detected X-ray flux at some level. In contrast, for most of the non-S-A UGC and ESO galaxies, the measured X-ray fluxes are clearly upper limits. Second, in each catalog it is evident that more E/S0 galaxies are detected than are spiral/irregular galaxies. Indeed, among the spiral/irregular galaxies, almost all of the X-ray detected galaxies are in the S-A; very few are in the UGC or ESO samples.

Our choice of $S/N = 2.5$ as the dividing line between detected and undetected galaxies in our survey comes from two results evident in these histograms. First, only $4/194 = 2\%$ of the blank fields have S/N values greater than 2.5. Second, the negative S/N tails of the blank fields and of the spiral/irregular UGC and ESO galaxy samples are well matched, indicating the galaxy observations have

a similar intrinsic S/N distribution as the blank fields. Based on the blank field observations, we would estimate that as many as 5 galaxies with fluxes near the S/N = 2.5 cutoff (2% of the detected sample) could have spurious detections.

4.2. Comparison to the Published Data

Fabbiano et al. (1992) have published Einstein observations for 405 individual galaxies, all of which are taken from the RC2 catalog. Given the format in which their data are published, we can compare the results of our survey with theirs in two ways: by count rate and by fully-corrected X-ray luminosity. For this comparison we find that we should exclude 22 galaxies from F92 that have only HRI observations, as we have used only IPC observations for our samples.

Upon further comparison, we find only 285 of the remaining 383 galaxies have quoted count rates and luminosities in common between both samples. Of the 98 galaxies that have F92 IPC observations but are not in our sample, almost all were excluded from our sample due to various objective selection criteria (e.g., size, diffuse emission, non-UGC/ESO/S-A, too short an image exposure). Ten galaxies are not in this comparison as they are among the few UGC galaxies not observed for the present survey.

In 112 of these 285 galaxies in common, both our data and those of F92 are upper limits. As comparing just the upper limit values for galaxy fluxes is inconclusive, this leaves us with 173 galaxies for which we can make a meaningful comparison with F92. Of these, 137 have detections in both data sets, 25 are detected by us and not by F92 and 11 are detected by F92 and not by us. Our survey has detected 251 galaxies (including those galaxies with and without radial velocities) at the 2.5σ level or higher. Thus, our sample contains 89 X-ray detected galaxies not previously published in the F92 compilation, a 43% increase over the 207 X-ray detected galaxies listed by F92.

That we have generally good agreement between our fully-corrected X-ray luminosities and those of F92 is shown in Figure 5 for the 137 galaxies detected in common between the two data sets. F92 fluxes have been adjusted to our distances for this comparison. As can be seen from Figure 5, while the relative flux scales between F92 fluxes and ours are the same, there are some differences in zero points. To examine this latter point more closely, Figure 6a shows the logarithm of the ratio of the F92 X-ray fluxes to our fluxes, plotted versus our X-ray fluxes, for galaxies detected by either data sample. The two dotted lines give the median values for $\log[L_X(\text{US})/L_X(\text{F92})]$ as a function of Hubble type

only for the galaxies detected by both surveys: -0.05 for E, S0 and I0 galaxies; -0.12 for spiral galaxies.

Such Hubble type-dependent differences can arise either from differences in energy range observed, or in HI-dependent correction for spectral energy distribution differences. To separate these two effects, in Figure 6b we plot the logarithm of the ratio of the observed count rates, $\log[C_t(\text{US})/C_t(\text{F92})]$ as a function of Hubble type, using the RC3 numerical code for Hubble type (see notes to Table 5a). The four galaxies detected in this survey with fluxes and countrates that differ significantly from those of F92 are noted by NGC number. In Figure 6b the dotted lines correspond to the median log ratios of count rates, U_s to $F92$, of -0.12 for E, S0 and I0 galaxies and -0.10 for S0 and spiral galaxies. To an accuracy of 0.01 dex, our count rates differ from those of F92 by 0.1 dex, in the sense of our count rates being lower.

We thus see that the differences between our fluxes and those of F92 are a combination of differences in observed count rates and differences in conversion of counts to flux. That our observed count rate is systematically lower than that of F92 is to be expected as we used a different energy range with the IPC than they did: F92 is quoted as using 0.2 to 4.0 keV; we use 0.5 to 4.5 keV. Similarly, it is also the case that our final luminosities should differ somewhat from those quoted by F92 as well. F92 used a bremsstrahlung spectrum of 5 keV for the spirals and irregulars and a Raymond spectrum of 1 keV for the ellipticals and S0's. As explained previously (§2.2), for our sample we did not *a priori* distinguish among Hubble types as to the physical source(s) of their X-ray spectra in converting observed countrate to X-ray flux.

Of the four galaxies which show significantly different F92 fluxes than our measurements, NGC 2832, NGC 1399 and NGC 4406 are all elliptical galaxies whose measured X-ray flux can be influenced by emission from diffuse cluster gas. NGC 5850 is a spiral galaxy with relatively low count rate (0.0053 cts/sec). The sense of the difference, $U_s/F92$ is that in the case of the three elliptical galaxies, our measurements do not include any diffuse cluster gas, while in the case of the spiral galaxy, it is likely due to a small difference in how the background was treated.

Given the current uncertainty in the true X-ray energy distributions from galaxies, we accept that differences of ~ 0.1 dex can occur among quoted luminosities derived from the same data under different assumptions. Indeed, we find it comforting that, to a level of 0.1 dex, the X-ray fluxes measured by F92 and by us are consistent with each other. While we find 6 galaxies (3.5% of galaxies detected by one or the other survey) have significant discrepant fluxes

between the two data samples (including 2 upper limits), this is to be expected. Such differences can occur due to such problematic measurement issues as background flux estimation on the IPC images and possible confusion of cluster diffuse emission with galaxy emission. In both cases, our measurement technique differs enough from that used by F92 to lead to possible large differences in a few cases.

We believe our method of doing essentially X-ray aperture photometry with the Einstein data base is complimentary to the technique employed by F92. In that paper, following their previous studies, those authors dealt with the IPC and HRI images in an analogous manner as one would do CCD surface photometry of galaxies, including global mapping of the response function. In contrast, our technique is more akin to photoelectric aperture photometry, complete with determining the X-ray “sky background” separately for each object.

Checks also were made of our measurements against earlier compilations (e.g. Forman, Jones, & Tucker 1985; Roberts et al.) and very good consistency was found. However, for these comparisons we note that the same procedures, by a subset of the same authors, were used to derive the fluxes.

5. Summary

We have made an X-ray survey of the Einstein IPC images which contain galaxies found in three catalogs — the Shapley-Ames, the UGC and the ESO catalogs — selected according to well-defined objective criteria. The X-ray fluxes for a total of 1018 galaxies were obtained, 313 in the S-A catalog, 393 non-S-A galaxies in the UGC and 312 non-S-A ESO galaxies. Our manner of obtaining the X-ray fluxes is analogous to obtaining optical photoelectric measurements: We locate apertures of defined sizes at the optical positions of the galaxies, and sample background at symmetric areas of the IPC field. In this way, our analysis differs from that done by Fabbiano et al. (F92), for which the analogy of CCD-like surface photometry is more applicable.

For these galaxies we have assembled associated optical data and have assigned distances either according to direct measurements (Tully-Fisher for spirals and $D_n - \sigma$ for ellipticals) or to the velocity field model of Faber & Burstein (1988).

The accuracy of our X-ray fluxes has been checked in four independent ways. First, we also measured X-ray flux at 194 random IPC positions in the same manner as for our program galaxies. The signal-to-noise histogram of these

“blank” fields is reasonably Gaussian in distribution, with an offset (+0.095) in S/N and only four observations lying beyond the 2.5σ level. Hence, we choose the lower limit for an X-ray detection in this survey to be 2.5σ . Second, X-ray fluxes on 97 IPC images were measured independently by two of us. Third, the negative side of the S/N histogram of the blank fields matches well the negative side of the S/N histogram of the program galaxies with the least intrinsic X-ray flux — the spiral and irregular galaxies.

Fourth, we have made a quantitative comparison with the X-ray fluxes and count rates published by Fabbiano et al. for 173 galaxies in common for which a galaxy was detected in either one or both of the samples. This comparison shows that the published fluxes differ by ± 0.1 dex owing primarily to differences in the assumptions made for converting observed count rates to flux.

Altogether we have 251 galaxies with detected X-ray flux (at the 2.5σ level or higher), or 24.7% of the sample. Eighty-nine of the detected galaxies are new, not previously catalogued by F92. Based on the S/N distribution of “blank” fields, as many as 5 of the detections may be spurious, which yields a true detection rate of 22.6%. The majority of galaxies, 767 in this sample, have only upper limit X-ray values, a result anticipated at the start of this survey. S/N histograms of the galaxies, divided into broad Hubble type bins of E+S0+I0, S+Irr and by catalog, show the expected result that the S-A galaxies, being the nearest, are detected at a much higher rate than UGC or ESO galaxies. These data will be used in a subsequent paper to revisit issues pertaining to X-ray flux generation in galaxies.

This research was supported by a NASA Grant NAG8-665 and 8-734 and by an ASU Faculty Grant-in-Aid to DB. APM was supported by NASA JOVE grant NAG8-264. The hospitality of the Center for Astrophysics is gratefully acknowledged, as well as the assistance of the Einstein data reduction team. This research has made use of the NASA/IPAC Extragalactic Database (NED) which is operated by the Jet Propulsion Laboratory, California Institute of Technology, under contract with the National Aeronautics and Space Administration. CJF and WRF acknowledge support from the Smithsonian Institution and the AXAF Science Center (NASA contract NAS8-39073).

REFERENCES

Aaronson et al. 1982, *ApJS* 50, 241

Burstein, D., Haynes, M.P. & Faber, S.M. 1991, *Nature* 353, 515

Burstein, D. & Heiles, C., 1984, *ApJS* 54, 33

Burstein, D., Willick, J.A. & Courteau, S. 1995, in *Opacity of Spiral Disks*, ed. J.I. Davies & D. Burstein, (Dordrecht: Kluwer), p. 73

Canizares, C. R., Fabbiano, G. & Trinchieri, G., 1987, *ApJ* 312, 503

Courteau, S. 1992, Ph.D. Thesis, U.C. Santa Cruz

Davies, J.I., Jones, H. & Trewhella, M. 1995, in *Opacity of Spiral Disks*, ed. J.I. Davies & D. Burstein, (Dordrecht: Kluwer), p. 85

de Vaucouleurs, G., de Vaucouleurs, A. & Corwin, H. G., 1976, *Second Reference Catalogue of Bright Galaxies* (Austin: University of Texas Press); (RC2)

de Vaucouleurs, G., de Vaucouleurs, A., Corwin, H. G., Buta, R. J., Paturel, G. & Fouqué, P., 1991, *Third Reference Catalogue of Bright Galaxies* (New York: Springer-Verlag); (RC3)

Dressel, L. L. & Condon, J. J., 1976, *ApJS* 31, 187

Fabbiano, G., Kim, D.-W. & Trinchieri, G., 1992, *ApJS* 80, 531 (F92)

Fabbiano, G. & Trinchieri, G., 1987, *ApJ* 315, 46

Faber, S. M. & Burstein, D., 1988, in *large-scale Motions in the Universe*, eds. V. C. Rubin and G. V. Coyne, Princeton U. Press (Princeton: NJ), p. 115

Faber, S. M., Wegner, G., Burstein, D., Davies, R. L., Dressler, A., Lynden-Bell, D., & Terlevich, R. J., 1989, *ApJS* 69, 763

Forman, W., Jones, C. & Tucker, W., 1985, *ApJ* 277, 19

Giovanelli, R. 1995, in *Opacity of Spiral Disks*, ed. J.I. Davies & D. Burstein, (Dordrecht: Kluwer), p. 127

Han, M.S. & Mould, J.R. 1992, *ApJ* 396, 453

Harris et al., 1991, *The Einstein IPC Source Catalog*

Huchra, J., 1976, *AJ* 81, 952

Lauberts, A. & Valentijn, E. A., 1989, *The Surface Photometry Catalogue of the ESO-Uppsala Galaxies*, (Garching-bei-München: European Southern Observatory)

Lauberts, A. 1982, The ESO/Uppsala Survey of the ESO (B) Atlas, (Garching-bei-München: European Southern Observatory) (ESO)

Long, K. S. & Van Speybroeck, L. P., 1981, in Accretion-Driven X-Ray Sources, ed. W. Lewin & E. P. J. van den Heuvel (Cambridge: Cambridge Univ. Press), 117

Marshall, F.J. & Clark, G.W. 1984, *ApJ* 287, 633

Mathewson, D.L., Ford, V.I. & Buchhorn, M. 1992, *ApJS* 81, 413

Nilson, P., 1973, Uppsala General Catalogue of Galaxies, *Nova Acta R. Soc. Sci. Uppsala*, ser. V:A, Vol. 1

Roberts, M. S., Hogg, D. E., Bregman, J. N., Forman, W. R. & Jones, C., 1991, *ApJS* 75, 751

Sandage, A. & Tammann, G. A., 1981, A Revised Shapley-Ames Catalogue of Bright Galaxies (Washington D.C.: Carnegie Institution of Washington)

Shapley, H. & Ames, A. 1932, *Ann. Harvard Coll. Obs.* 88, No. 2 (S-A)

Stark et al. 1992, *ApJS* 79, 77

Tormen, G. & Burstein, D. 1995, *ApJS* 96, 123 and references therein

Valentijn, E.A. 1990, *Nature* 346, 153

Willick, J.A., Courteau, S., Faber, S.M., Burstein, D., & Dekel, A. 1995, *ApJ* 446, 12

Willick, J.A., Courteau, S., Faber, S.M., Burstein, D., Dekel, A., & Kolatt, T. 1996a, *ApJ* 457, 460

Willick, J.A., et al, 1996b, *ApJ*, in press.

Zwicky, F., Herzog, E., Kowal, C.T., Wild, P. & Karpowicz, M. 1961, 1963, 1965, 1966, 1968a,b, Catalogue of Galaxies and Clusters of Galaxies, in six volumes (Pasadena: California Institute of Technology)

Figure Captions

Figure 1. The fraction of galaxies surveyed in each of the three catalogs used for this survey: a) Shapley-Ames (SA); b) Uppsala General Catalog (UGC); and c) European Southern Catalog (ESO). In each case, the galaxies are divided by Hubble types: E+S0+S0/a galaxies (closed squares); early-type spiral galaxies (open circles); late-type spirals + irregulars (open squares) and multiple/double/peculiar galaxies (open triangles; only in b) and c)). The fraction of galaxies in our survey in the SA catalog are plotted as a function of apparent magnitude. For both the UGC and ESO catalogs, they are plotted as a function of log diameter in arcmin.

Figure 2. The distribution of calculated IPC S/N of the 194 “blank” fields, randomly selected as being free of obvious X-ray emission on the program IPC fields, and reduced in the same manner as the program measurements. The distribution is very close to being Gaussian, with a small net offset of 0.095 in S/N.

Figure 3. a) — d) The IPC S/N distributions for E+S0 galaxies for each of the three optical catalogs (a,b,c) plus the three catalogs combined (d). In each case, the S/N histogram obtained from the 194 blank fields is overplotted (dotted line). Note the good match of the negative tails of the S/N distributions of the blank fields and program fields for the UGC and ESO samples.

Figure 4 a) — d) IPC S/N distributions for the spiral and irregular galaxies in each of the three optical catalogs (a,b,c) plus the three catalogs combined (d). See Figure 3 for details.

Figure 5. F92 X-ray luminosities plotted versus our X-ray luminosities for 137 galaxies detected in common between our two surveys. Closed circles are X-ray luminosities for E and S0 galaxies; closed squares are early-type spirals and closed triangles are late-type spirals and irregulars.

Figure 6. a) The logarithm of the ratio of X-ray luminosity as determined in this survey ($L_X(Us)$) to that determined by F92 ($L_X(F92)$), plotted as a function of $\log L_X(Us)$. Closed symbols are detections in both surveys; open symbols are detections by Us but F92 upper limits; plus signs, x's and asterisks are detections by F92 but Us upper limits. Circles and asterisk are E galaxies; squares and plus signs are S0+I0 galaxies; triangles and crosses are spiral and irregular galaxies. The dotted lines mark the median log ratio for E+S0+I0 galaxies (-0.05) and S+I galaxies (-0.12). b) The logarithm of measured count rates, Us to F92, now plotted as a function of RC3 Hubble type number code. Median values for E+S0+I0 galaxies (-0.12) and for S+I galaxies (-0.10) are shown as dotted lines. Here solid squares are mutual detections, open squares

are detections by Us but F92 upper limits; open triangles are detections by F92 but Us upper limits.